

CHARACTERIZATION AND DEVICE PERFORMANCE OF (AgCu)(InGa)Se₂ ABSORBER LAYERS

Gregory M. Hanket, Jonathan H. Boyle, and William N. Shafarman
Institute of Energy Conversion, University of Delaware, Newark, DE 19716, U.S.A.

ABSTRACT

The study of (AgCu)(InGa)Se₂ absorber layers is of interest in that Ag-chalcopyrites exhibit both wider bandgaps and lower melting points than their Cu counterparts. (AgCu)(InGa)Se₂ absorber layers were deposited over the composition range $0 < \text{Ag}/(\text{Ag}+\text{Cu}) < 1$ and $0.3 < \text{Ga}/(\text{In}+\text{Ga}) < 1.0$ using a variety of elemental co-evaporation processes. Films were found to be single-phase over the entire composition range, in contrast to prior studies. Devices with Ga content $0.3 < \text{Ga}/(\text{In}+\text{Ga}) < 0.5$ tolerated Ag incorporation up to $\text{Ag}/(\text{Ag}+\text{Cu}) = 0.5$ without appreciable performance loss. Ag-containing films with $\text{Ga}/(\text{In}+\text{Ga}) = 0.8$ showed improved device characteristics over Cu-only control samples, in particular a 30-40% increase in short-circuit current. An absorber layer with composition $\text{Ag}/(\text{Ag}+\text{Cu}) = 0.75$ and $\text{Ga}/(\text{In}+\text{Ga}) = 0.8$ yielded a device with $V_{\text{OC}} = 890$ mV, $J_{\text{SC}} = 20.5$ mA/cm², fill factor = 71.3%, and $\eta = 13.0\%$.

INTRODUCTION

Silver chalcopyrites exhibit bandgaps ~0.2 eV wider and melting points ~200 °C lower than their Cu counterparts. When widening bandgap through the alloying of various constituent elements into CuInSe₂-based absorber layers, Ag is unique in its simultaneous lowering, not increasing, of the melting point. Fig. 1 shows the bandgaps and melting points of the chalcopyrites formed by the substitution of Ag, Ga, and S into CuInSe₂, and the linearly-interpolated ranges of bandgap and melting point hypothetically achievable in the (AgCu)(InGa)Se₂ system. Specific motivations for studying the (AgCu)(InGa)Se₂ system are the development of wider bandgap devices, either as standalone devices with increased voltage or as the top cell in tandem structures, and the reduction of processing temperature, for reduced thermal budget or improved device performance on substrates such as polyimides.

The phase behavior of the (AgCu)(InGa)(TeSe)₂ system has been previously studied by Avon et al. [1] A miscibility gap was observed by x-ray diffraction (XRD) analysis of ampoule-synthesized (AgCu)(InGa)Se₂ ingots in the approximate composition window $0.25 < \text{Ag}/(\text{Ag}+\text{Cu}) < 0.75$ and $0.25 < \text{Ga}/(\text{In}+\text{Ga}) < 1.0$. [1] From a device standpoint, a noteworthy result in the Ag(InGa)Se₂ system is the work of Nakada et al. who achieved a device with $V_{\text{OC}} = 949$ mV, $J_{\text{SC}} = 17.0$ mA/cm², FF = 58%, and $\eta = 9.3\%$ using an Ag(In_{0.2}Ga_{0.8})Se₂ absorber layer. [2]

The present study includes results for solar cells spanning nearly the complete (AgCu)(InGa)Se₂ pentenary system. Erslev et al., collaborators in the present project, recently reported transient photocapacitance measurements that show sharper bandtails in (AgCu)(InGa)Se₂ devices than in Cu(InGa)Se₂ devices. [3] This suggests reduced structural disorder in the (AgCu)(InGa)Se₂ films which may be related to the melting point reduction. It was also found that Ag reduces the free carrier concentration by roughly an order of magnitude. Thus there may be a tradeoff between increased V_{OC} from the increased bandgap and reduced defect densities versus lower V_{OC} via reduced free carrier concentration.

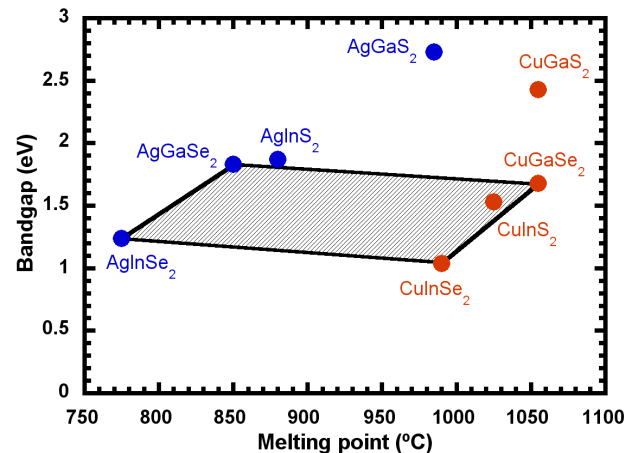


Fig. 1. Bandgaps and melting points of ternary Ag- and Cu-chalcopyrites. The grey quadrilateral describes the linearly-interpolated bounds of bandgap and melting point hypothetically achievable in the (AgCu)(InGa)Se₂ pentenary system.

In this paper we survey the phase behavior and device characteristics over a broad (AgCu)(InGa)Se₂ composition space using films deposited by elemental co-evaporation with time-invariant incident flux profiles. These results are used to determine candidate compositions for further V_{OC} or efficiency improvements via manipulation of the time-flux profiles.

EXPERIMENTAL

(AgCu)(InGa)Se₂ films were deposited at 2 μm thickness onto Mo-coated soda lime glass substrates by elemental co-evaporation in the composition space $0 < \text{Ag}/(\text{Ag}+\text{Cu}) < 1$ and $0.3 < \text{Ga}/(\text{In}+\text{Ga}) < 1.0$. Films were deposited using

two flux-time profiles: “single-stage” deposition in which incident flux profiles were held constant over a 60-minute deposition; and “three-stage” deposition where In and Ga were deposited for 30 minutes, then Ag and Cu were deposited over 50 minutes, followed by a final ~15 minute In and Ga deposition. In all cases the relative Ag-to-Cu and Ga-to-In incident flux ratios were constant for a given film, and Se was delivered in stoichiometric excess. Depositions were performed at a substrate temperature $T_{SS} = 550^{\circ}\text{C}$. $(\text{Ag}+\text{Cu})/(\text{In}+\text{Ga})$ ratios were in the range $0.8 < (\text{Ag}+\text{Cu})/(\text{In}+\text{Ga}) < 0.9$. A systematic attempt to examine the $(\text{Ag}+\text{Cu})/(\text{In}+\text{Ga})$ single-phase existence region or the effect of $(\text{Ag}+\text{Cu})/(\text{In}+\text{Ga})$ ratio on device performance was not attempted.

Films were characterized for composition by energy dispersive x-ray spectroscopy (EDS), and crystallographically by symmetric x-ray diffraction (XRD) using $\text{CuK}\alpha_1$ incident radiation.

Devices were fabricated by chemical bath deposition of 400-500 Å CdS, followed by RF sputter deposition of 500Å i-ZnO/1500 Å ITO, e-beam deposition of Ni-Al grids, and finally delineation by mechanical scribing to individual devices with area 0.47cm^2 . Devices were characterized by J-V analysis and spectral response measurements. Selected devices further received a 1100 Å MgF_2 anti-reflection (AR) coating.

RESULTS AND DISCUSSION

Phase behavior in $(\text{AgCu})(\text{InGa})\text{Se}_2$ films

Single-stage films were deposited over a broad composition range (see Fig. 2) to survey phase behavior, optical properties [4], and device performance. XRD analysis in the present study, in contrast to the earlier work of Avon [1], indicated little evidence of chalcopyrite phase segregation. For example, a film deposited with composition $\text{Ag}/(\text{Ag}+\text{Cu}) = 0.46$ and $\text{Ga}/(\text{In}+\text{Ga}) = 0.50$, near the center of the two-phase region reported by Avon et al., showed no evidence of phase segregation as shown by the XRD (112) peak profile in Fig. 3. A possible explanation for the discrepancies between the two bodies of data is that the films in the present study are in a state of metastable miscibility, as they were deposited at $T_{SS} = 550^{\circ}\text{C}$ compared to the ampoule annealing temperatures of $600 - 800^{\circ}\text{C}$ used by Avon. Another possible explanation is that the thermodynamics of the present films are sufficiently different from the bulk thermodynamics that phase behavior is affected.

Device performance of single-stage $(\text{AgCu})(\text{InGa})\text{Se}_2$ absorber layers

Fig. 4 summarizes the device characteristics exhibited by single-stage absorber layers. Selected samples from this series of single-stage films were analyzed by Erslev et al.[3] At compositions $0.3 < \text{Ga}/(\text{In}+\text{Ga}) < 0.5$ and

$\text{Ag}/(\text{Ag}+\text{Cu}) < 0.5$, the presence of Ag does not substantially influence device parameters at a given Ga content. Above $\text{Ag}/(\text{Ag}+\text{Cu}) > 0.5$, J_{SC} begins to drop, presumably due to the bandgap increase, without an accompanying increase in V_{OC} . As Ga content further increases past $\text{Ga}/(\text{In}+\text{Ga}) > 0.5$, V_{OC} in the $(\text{AgCu})(\text{InGa})\text{Se}_2$ devices fails to scale linearly with increasing bandgap, similar to well established behavior in the $\text{Cu}(\text{InGa})\text{Se}_2$ system, [5] and overall device efficiency correspondingly decreases. These results are noteworthy, however, in that they demonstrate a high tolerance to Ag incorporation from a device standpoint.

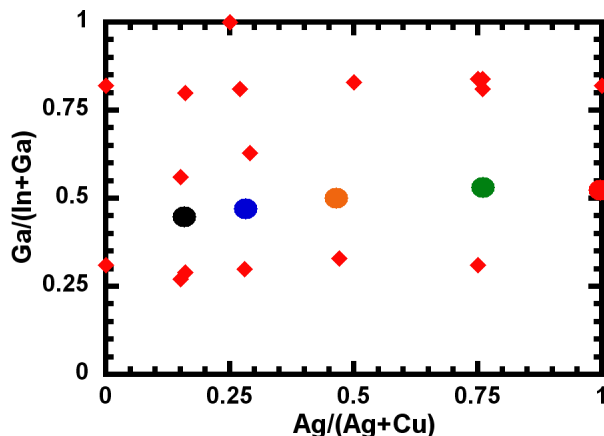


Fig. 2. $(\text{AgCu})(\text{InGa})\text{Se}_2$ composition summary map of single-stage films deposited during the present study. XRD (112) line profiles for films with $\text{Ga}/(\text{In}+\text{Ga}) \sim 0.5$ (denoted by colored circles) are shown in Fig. 3.

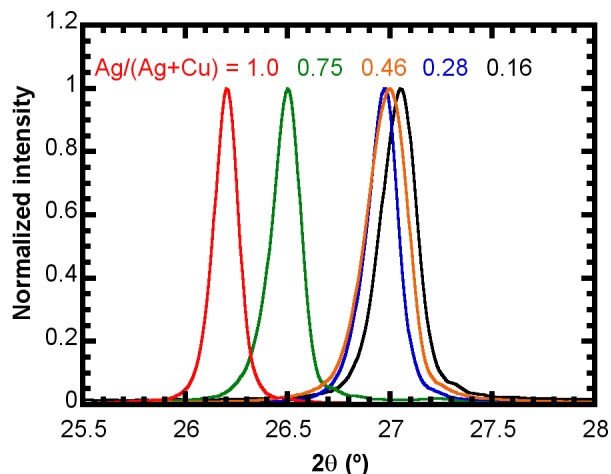


Fig. 3. XRD (112) line profiles for films with $\text{Ga}/(\text{In}+\text{Ga}) \sim 0.5$ denoted in Fig. 2. No obvious evidence of phase segregation is observed in contrast to earlier reports [1].

As the Ga content further increases to $\text{Ga}/(\text{In}+\text{Ga}) = 0.8$, the addition of Ag over the broad range $0.15 < \text{Ag}/(\text{Ag}+\text{Cu}) < 0.75$ results in a marked improvement in virtually all device parameters. In particular, J_{SC} increases from 12-13 mA/cm^2 to $\sim 17 \text{mA}/\text{cm}^2$, resulting in an overall η increase

from ~5% to 8-9%. Fill factor also generally increases with Ag incorporation. Cu- and In-free films exhibit poor device behavior, though these data are limited. Device results selected for high efficiency and wide bandgap are shown in Table 1. The highest-efficiency device over the entire course of the present study is the sample with $\text{Ag}/(\text{Ag}+\text{Cu}) = 0.15$ and $\text{Ga}/(\text{In}+\text{Ga}) = 0.45$, yielding $V_{\text{OC}} = 709$ mV, $J_{\text{SC}} = 32.3$ mA/cm², FF = 76.9% and $\eta = 17.6\%$. The highest V_{OC} obtained with a single-stage absorber layer was $V_{\text{OC}} = 870$ mV for a film with composition $\text{Ag}/(\text{Ag}+\text{Cu}) = 0.75$ and $\text{Ga}/(\text{In}+\text{Ga}) = 0.8$.

Wide-bandgap absorber layers deposited by three-stage deposition

Based upon generally observed improvements in $\text{Cu}(\text{InGa})\text{Se}_2$ device performance, and Nakada's use of a three-stage process for depositing wide bandgap $\text{Ag}(\text{InGa})\text{Se}_2$ devices [2], $(\text{AgCu})(\text{InGa})\text{Se}_2$ absorber layers were deposited by a three-stage process. A series of films were deposited with fixed $\text{Ga}/(\text{In}+\text{Ga}) = 0.8$, and $\text{Ag}/(\text{Ag}+\text{Cu}) = 0, 0.25, 0.5, 0.75$, and 1.0 .

Fig. 5 shows the J-V curves for the best device at each Ag content, with Table 2 showing the corresponding J-V characteristics. The $\text{Ag}(\text{GaIn})\text{Se}_2$ film delaminated in the CdS bath, so could not be characterized. Device efficiency increases with Ag content, though this cannot be attributed to the monotonic increase of any single device parameter. The highest V_{OC} , fill factor, and efficiency were obtained for the $\text{Ag}/(\text{Ag}+\text{Cu}) = 0.75$ absorber layer, which yielded device parameters $V_{\text{OC}} = 871$ mV, $J_{\text{SC}} = 19.7$ mA/cm², FF = 68.0, and $\eta = 11.7\%$. This absorber layer had the same composition as the highest- V_{OC} single-stage film – $\text{Ag}/(\text{Ag}+\text{Cu}) = 0.75$ and $\text{Ga}/(\text{In}+\text{Ga}) = 0.8$. While V_{OC} and FF were equivalent, the current increased from 15.2 to 19.7 mA/cm² in the transition from the single-stage to three-stage process. Fig. 6 shows the spectral response measurements for the three-stage films, and indicates that Ag appears very effective at increasing current collection in general, and long wavelength current collection in particular. Improved long wavelength collection would be consistent with increased depletion widths resulting from reduced free carrier concentrations.[3] Three-stage films have not yet been subjected to a detailed device analysis, so the mechanism responsible for the performance difference between single-stage and three-stage absorber layers is unknown.

The variation between the V_{OC} s for the highest efficiency devices in Table 2 and highest- V_{OC} devices denoted in Fig. 6 suggest that the absorber deposition process requires refinements to improve the robustness. Nonetheless, these results on a limited number of samples justify further efforts.

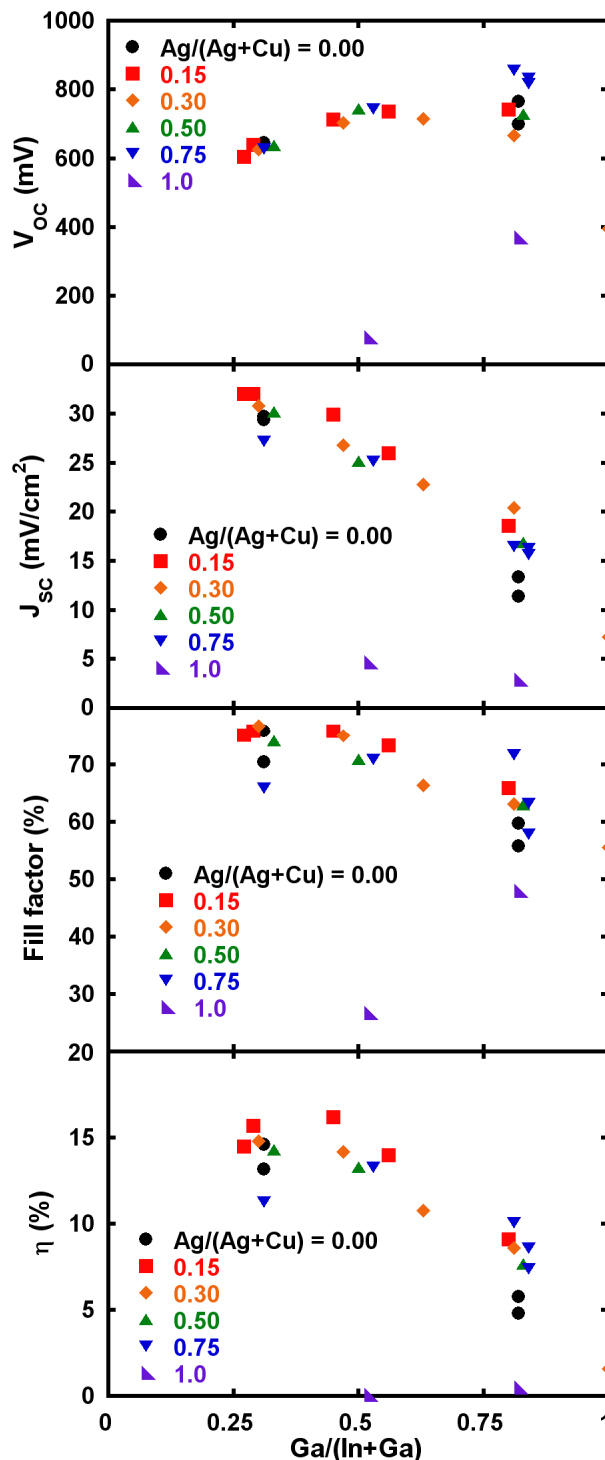


Fig. 4. J-V characteristics of devices fabricated from single-stage $(\text{AgCu})(\text{InGa})\text{Se}_2$ absorber layers over the course of the present study.

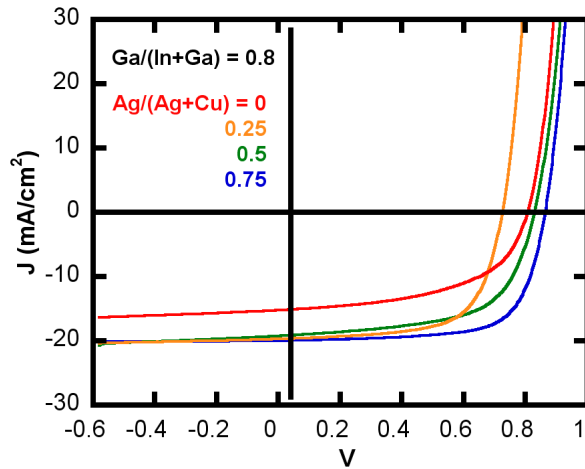


Fig. 5. J-V curves corresponding to devices in Table 2. While overall device efficiency increases with Ag content, it cannot be ascribed to a monotonic increase in a single device parameter.

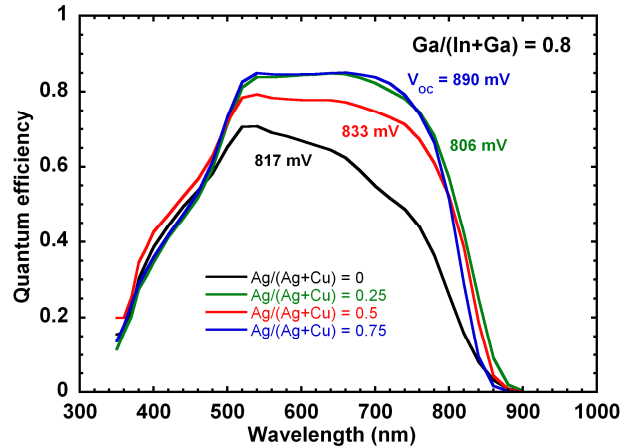


Fig. 6. Spectral response measurements of high-bandgap (AgCu)(InGa)Se₂ devices deposited by a three-stage process. Maximum V_{oc}s observed at a given composition, irrespective of the accompanying spectral response curves, are indicated and are generally consistent with increasing bandgap indicated by the band edge measured at QE = 0.2. Poor long-wavelength current collection of the Cu(InGa)Se₂ device precludes even a qualitative bandgap estimate.

Table 1. J-V characteristics of selected devices fabricated from single-stage (AgCu)(InGa)Se₂ absorber layers.

$\frac{\text{Ag}}{\text{Ag} + \text{Cu}}$	$\frac{\text{Ga}}{\text{In} + \text{Ga}}$	E _g (eV)	V _{oc} (mV)	J _{sc} (mA/cm ²)	FF (%)	η (%)
0.15	0.45	1.31	716	29.9	76.0	16.3
			709 [†]	32.3 [†]	76.9 [†]	17.6 [†]
0.75	0.80	1.63	870	15.2	68.8	9.1

[†]With 1100Å MgF₂ AR coating.

Table 2. Best-efficiency characteristics for three-stage absorber layers with Ga/(In+Ga) = 0.8 deposited at 550°C.

Ag/(Ag+Cu)	E _g (eV)	V _{oc} (mV)	J _{sc} (mA/cm ²)	FF (%)	η (%)
0	1.54	806	15.2	53.8	6.6
0.25	1.53	724	19.7	65.9	9.4
0.50	1.54	828	19.2	61.3	9.8
0.75	1.6	871	19.7	68.0	11.7

Comparison to other wide-bandgap CIS-based devices

A continuing difficulty in the development of wide bandgap CuInSe₂ based devices has been the failure of V_{OC} to scale with bandgap. The highest-efficiency wide bandgap device in the present study (the highest efficiency device in Table 2), after AR coating, is compared to other published results in Table 3. V_{OC} of the (AgCu)(InGa)Se₂ device falls 15 mV short of the CuGaSe₂ device [6], but exhibits 39% higher J_{SC} and a concurrent 37% relative efficiency increase. While failing to match the V_{OC} of Nakada, the (AgCu)(InGa)Se₂ fill factor is 71% compared to 58% for the Ag(InGa)Se₂ device, resulting in a marked efficiency improvement. Compared to the other higher efficiency devices ($\eta > 10\%$) present in the table, the (AgCu)(InGa)Se₂ device exhibits V_{OC} of 60 mV or greater. These results suggest that Ag incorporation may be an effective means of increasing V_{OC} without the detrimental effect on the other device parameters that is typically observed at bandgaps > 1.5 eV.

CONCLUSIONS

A number of conclusions can be drawn from the present data. The first broad observation is that the (AgCu)(InGa)Se₂ system appears highly tolerant to large

degrees of Ag incorporation in terms of both phase behavior and device performance. The single-phase composition region under typical photovoltaic thin film deposition conditions may be much broader than previously reported for ingots.[1] This has potential implications for improved film growth at lower temperatures by incorporation of significant quantities of Ag and a corresponding reduction in melting point. Second, Ag appears effective in improving device characteristics, J_{SC} in particular, for absorber layers with Ga/(In+Ga) > 0.5 , provided that some Cu and In remain present in the film. A wide bandgap device with Ag/(Ag+Cu) = 0.75 and Ga/(In+Ga) = 0.8 that yielded a device with V_{OC} = 890 mV, J_{SC} = 20.5 mA/cm², FF = 71.3%, and $\eta = 13.0\%$ surpasses the performance of other wide bandgap alloys. It is hypothesized that (AgCu)(InGa)Se₂ film composition and deposition process may be optimized for specific desired outcomes: maximized cell efficiency, increased V_{OC} to reduce module series resistance losses, maximum V_{OC} for tandem devices, or reduced temperature deposition for low temperature substrates or simplified glass handling. Further work is necessary to determine whether the (AgCu)(InGa)Se₂ alloy system can meet these desired objectives, as well as to address such issues as device reproducibility and stability.

Table 3. Selected high-bandgap devices in order of increasing V_{OC}.

Material	E _g (eV)	V _{oc} (mV)	J _{sc} (mA/cm ²)	FF (%)	η (%)	Group
Cu(InAl)Se ₂	1.51	750	20.1	65.8	9.9	IEC[7]
Cu(InAl)Se ₂	1.66	760	16.7	61.5	7.8	IEC[7]
Cu(InGa)S ₂	1.53	770	21.6	73.7	12.3	HMI[8]
Cu(InGa)(SeS) ₂	1.5	770	20.6	75.3	11.9	IEC[9]
Cu(InGa)S ₂	-	830	20.9	69.1	12.0	FSEC[10]
(AgCu)(InGa)Se₂	1.6	890	20.5	71.3	13.0	IEC
CuGaSe ₂	1.68	905	14.9	70.8	9.5	NREL[6]
Ag(InGa)Se ₂	1.7	949	17.0	58	9.3	AGU[2]

ACKNOWLEDGMENTS

This material is based upon work supported by the Department of Energy under Award Number DE-FG36-08GO18019.

Disclaimer

This report was prepared as an account of work sponsored by an agency of the United States Government. Neither the United States Government nor any agency thereof, nor any of their employees, makes any warranty, express or implied, or assumes any legal liability or responsibility for the accuracy, completeness, or usefulness of any information, apparatus, product, or process disclosed, or represents that its use would not infringe privately owned rights. Reference herein to any specific commercial product, process, or service by trade name, trademark, manufacturer, or otherwise does not necessarily constitute or imply its endorsement, recommendation, or favoring by the United States Government or any agency thereof. The views and opinions of authors expressed herein do not necessarily state or reflect those of the United States Government or any agency thereof.

REFERENCES

- [1] Avon et al., *J. Appl. Phys.* **55** (2), 1984, p. 524.
- [2] Nakada et al., *Mater. Res. Soc. Symp. Proc.* **865**, 2005, p. F11.1.1.
- [3] Erslev et al., MRS Spring Meeting, Apr. 13-17, San Francisco, CA, 2009, to be published.
- [4] Boyle et al., 34th IEEE PVSC, to be published.
- [5] W.N. Shafarman, R. Klenk, and B.E. McCandless, *J. Appl. Phys.* **79**, 1996, p. 7324.
- [6] Young et al., *Prog. Photovolt.: Res. Appl.* **11**, 2003, p. 535.
- [7] Shafarman et al., *Proc. 29th IEEE PVSC*, 2002, p 519.
- [8] R. Kaigawa, et al., *Thin Sol. Films* **415**, 2002, p. 266.
- [9] Nishiwaki, S. and William Shafarman, *Proc. IEEE 4th WCPEC*, 2007, p. 461.
- [10] Noufi et al., *Proc. IEEE 4th WCPEC*, 2007, p. 317.